Current Applied Physics 16 (2016) 1349–1352

Contents lists available at ScienceDirect

Current Applied Physics

journal homepage: www.elsevier.com/locate/cap

Effect of microstructures on the Gilbert damping in Co/Ni multilayers

Hyon-Seok Song [a], Kyeong-Dong Lee [c], See-Hun Yang [d], Jeong-Woo Sohn [a, b], Hyun Joong Kim [a], Chun-Yeol You [a], Byong-Guk Park [c], Stuart Parkin [d], Sung-Chul Shin [a, b], Jung-Il Hong [a, e, *]

[a] Department of Emerging Materials Science, DGIST, Daegu, 42988, South Korea
[b] Department of Physics and CNSM, KAIST, Daejeon, 34141, South Korea
[c] Department of Materials Science and Engineering, KAIST, Daejeon, 34141, South Korea
[d] IBM Research Division, Almaden Research Center, San Jose, CA, 95120, USA
[e] DGIST Research Center for Emerging Materials, DGIST, Daegu, 42988, South Korea

ARTICLE INFO

Article history:
Received 4 June 2016
Received in revised form
24 July 2016
Accepted 1 August 2016
Available online 3 August 2016

Keywords:
Multilayers
Gilbert damping
Anisotropy
Microstructure

ABSTRACT

Proper understanding of spin dynamics in the magnetic multilayer system is a necessary step for the fabrication of practical magnetic devices. In the present study, spin dynamics in the $[Co/Ni]_N/Ti$ multilayers at various Co and Ni layer thicknesses were obtained by optical method with the aim to identify the structural effects on the Gilbert damping constant of the multilayer system. It was found that the change of crystallinity and magnetocrystalline anisotropy depending on the relative thicknesses ratio of Co and Ni layers work as the main factor to determine the Gilbert damping behavior.

There have been many investigations on spin dynamics described traditionally by Landau–Lifshitz–Gilbert (LLG) equation, which considers spin torques from various external sources and their relaxations via Gilbert damping. After Slonczewski [1] proposed a new type of toque called Spin-Transfer Torque (STT) in 1996, many additional torque terms have been introduced and classified, such as field-like torque and damping-like torque [2]. Studies on these new findings have driven many new spintronics applications that require energetic torque mechanism in nanostructures as well as low Gilbert damping.

While various types of toque have been proposed and received considerable attentions in recent years, investigation on Gilbert damping retains its own importance with the consideration of not only its underlying energy-related characteristics of magnetic dissipation behavior but also the possible relationships to other magnetic parameters. Furthermore, Gilbert damping term is the most dominant first order term in LLG equation. It is noteworthy to recognize that the Gilbert damping term is still the governing factor in the consideration of spin dynamics. Most representative and well known applications include the race track memory using the domain wall motion [3] and Skyrmions [4], and spin-transfer torque magnetic random access memory (STT-MRAM) [5]. For the realization of high density STT-MRAM, reducing the critical switching current density, J_c, is essential, and it is well known that J_c varies in proportion to the Gilbert damping constant α [6]. Current density control in a race track memory is also critically related to α [4]. Therefore, there have been continuous attempts to understand and control the Gilbert damping in magnetic thin films. Finding a correlation between the Gilbert damping and other magnetic properties, such as magnetic anisotropy [7–9], material compositions in various magnetic materials, e. g. Fe_xCo_{1-x} [10], Ni-Fe or Ni-Co [11] and Fe-Co-Ni [12] alloys, and the crystallinity of magnetic films, is a task with both academic and technical demands, yet it remains as a challenging issue.

In the previous works, α in Co/Ni multilayers was investigated by varying the structural properties, for example the stack number [13] and Ti-buffered layer thickness [8]. In these cases, it was found that perpendicular magnetic anisotropy (PMA) increased as the stack number and Ti-buffered layer thickness increases. However, the relationships between PMA and α turned out to be different in each case. Because PMA arises not only from spin orbit coupling but

* Corresponding author. Department of Emerging Materials Science, DGIST, Daegu, 42988, South Korea.
E-mail address: jihong@dgist.ac.kr (J.-I. Hong).

http://dx.doi.org/10.1016/j.cap.2016.08.001
1567-1739/

Table 1
Ratios of Ni to Co thickness and their saturation fields in Co/Ni multilayers.

t_{Ni}/t_{Co}	t_{Ni} (Å)	t_{Co} (Å)	H_s (Oe)
1.67	5	3	1810
2	6	3	2140
2.33	7	3	1720
2.5	5	2	2000
2.67	8	3	2090
3	6	2	2260
4	8	2	3800
6	6	1	3340

also from other factors such as dipolar interaction [14] or the difference in orbital moments between perpendicular and in-plane magnetization axis [15], systematic investigations on Gilbert damping are required for clear and comprehensive understanding.

In the present study, we investigate the Gilbert damping of Co/Ni multilayers. It is considered to be an emerging material in spintronics device applications with its advantage of low switching current density and strong thermal stability [16]. We measured the damping parameter α using an all-optical method as the Co and Ni layer thicknesses were varied as in Table 1 to find out the relationships between the material concentration and Gilbert damping. Comparison with the previous results in Ref. [8,13] were made for clearer understandings.

Co/Ni multilayer films were prepared on a Si/SiO_2 (001) substrate by magnetron sputtering with a base pressure of 5×10^{-9} Torr. The stack structure of the sample series is Ti (60 Å)/Co (3 Å)/[Ni (t_{Ni} Å)/Co (t_{Co} Å)]$_6$/TaN (50 Å). t_{Ni} and t_{Co} were varied as shown in Table 1. The ratio between Ni and Co thicknesses, t_{Ni}/t_{Co}, ranged from 1.67 to 6. Polar magneto-optical Kerr effect (p-MOKE) and vibrating sample magnetometer (VSM) was employed to measure the magnetic properties of the samples. Fig. 1(a) shows the hysteresis loops measured by p-MOKE at room temperature. As shown in Fig. 1(b), measured magnetic coercivity H_c increased as t_{Ni}/t_{Co} increases. Saturation magnetization field H_s was obtained from the hysteresis loop measured along the hard axis with VSM as shown in Fig. 1(b).

Measurements of α were carried out using the time-resolved MOKE [13]. A Kerr-lens mode-locked Ti:Sapphire oscillator generates laser pulses whose center wavelength are ~800 nm. The laser pulse has a repetition rate of 82 MHz and a pulse width of 30 fsec. We doubled the frequency of the probe beam with a BBO crystal. The laser beam was then split into a pump beam and a probe beam. The probe beam intensity was considerably weaker than that of the pump beam (1:200). The pump and probe beams were then fed into a polarization-conserving objective lens (50×, 0.5 numerical aperture). The probe beam was incident along the normal axis of the sample plane. The spot diameters of the pump and probe beams were ~2 μm and ~1 μm, respectively. The thermal effect from the pump beam was checked by changing the pump fluence F in the range of 2.5–8.8 mJ/cm^2. As shown in Fig. 2, it was confirmed that the transient heating effect was ignorable within the experimental error. To reduce the noise, we used balanced detection and lock-in amplifier filtering via mechanical chopping on the pump beam at 1300 Hz. The external magnetic field H was applied with the angle θ_H of 60° from the normal axis of the sample plane [8,13].

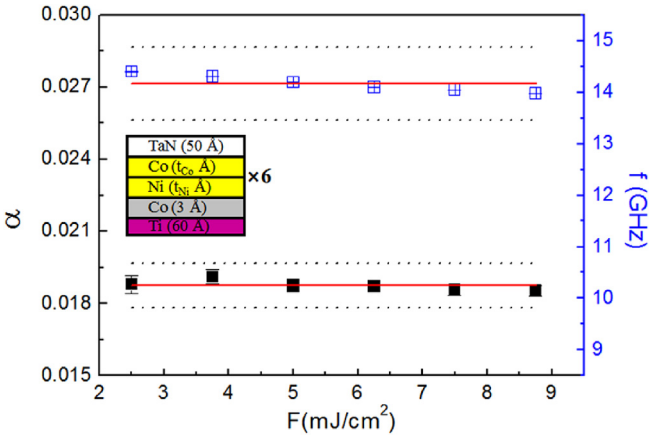

Fig. 2. Gilbert damping α(black solid symbols) and resonance frequency f(blue open symbols) as a function of the pump fluence F when $t_{Ni}/t_{Co} = 1.67$. Red line indicates the average value and Block dotted lines indicates the average value with 5% error. Note that the error bar is about the size of the data symbol. The inset shows the Co/Ni multilayer structure. (For interpretation of the references to colour in this figure legend, the reader is referred to the web version of this article.)

Fig. 3 shows the time-resolved MOKE data of two representative samples with $t_{Ni}/t_{Co} = 1.67$ and 6, under the conditions of $H = 5.6$ kOe, $\theta_H = 60°$, and $F = 5$ mJ/cm^2. The Kerr signals were fitted to a damped-harmonic function expressed as $\theta = \theta_0 + Ae^{-t/t_0} + Be^{-t/\tau}\sin(2\pi ft + \varphi)$ [17]. The first term θ_0 represents the offset background, the second term is the remagnetization with relaxation time t_0, and the final term is the precessional motion with the resonance frequency f, the relaxation time τ, and the initial phase φ. The solid curves in Fig. 3 are fitted lines. When t_{Ni}/t_{Co} is larger, precessional motion disappear faster meaning that it has a greater damping constant. Fig. 4(a) shows f as a function of H with $t_{Ni}/t_{Co} = 2.67$. Here, $\theta_H = 30°$ and $F = 5$ mJ/cm^2. The value of f increases with H, which is well explained by the Kittel formula, $f = (\gamma/2\pi)\sqrt{H_1 H_2}$ where $H_1 = H\cos(\theta_H - \theta) + H_k\cos^2\theta$ and

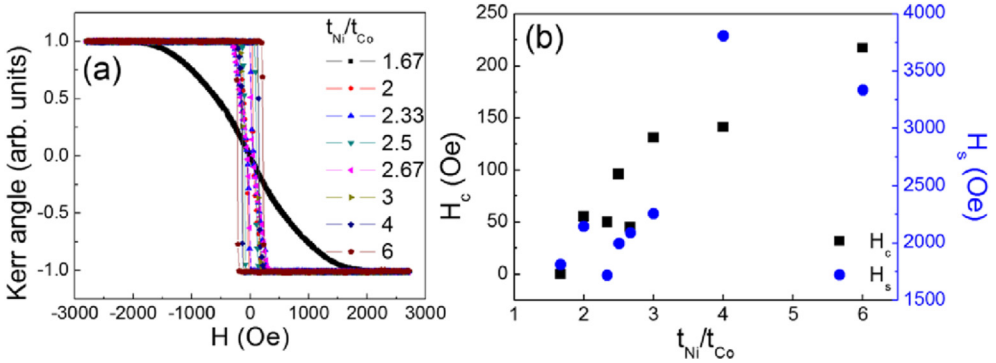

Fig. 1. (a) Magnetic hysteresis loop measured by p-MOKE with ratio between Ni and Co thickness, $t_{Ni}/t_{Co} = 1.67$–6. (b) Coercivity field H_c(squared symbols) and saturation field H_s(circular symbols) as a function of t_{Ni}/t_{Co}, which is determined by p-MOKE and VSM.